

Formation of layered nanofibric materials and composite coatings

J. M. Khakkulov*, Z. Sh. Temirov*, B. M. Matyakubov ^{*,†,‡} and A. P. Sultanov*

**National University of Uzbekistan named after Mirzo Ulugbek,
Tashkent, 100174, Republic of Uzbekistan*

*†University of Public Safety of the Republic of Uzbekistan,
Tashkent, 100109, Republic of Uzbekistan*

‡matyakubov-bekzod@mail.ru

Received 16 August 2023

Revised 27 October 2023

Accepted 5 November 2023

Published 11 January 2024

Using an electrospinning device, we determined the optimal conditions for producing nanofibers from a 10% solution of Co-AN. These conditions involved applying a 15 kV voltage to the anode, which was connected to the syringe containing the solution, and maintaining a distance of 12–15 cm from the needle tip to the collector screen (cathode). The filament diameter (d) ranged from 0.2 to 0.5 mm. This setup allowed the formation of nanofibers under the cover. The electrolysis process was conducted for varying durations, ranging from 4 to 14 h, while applying currents of 2 mA, 4 mA, and 8 mA. At 4 mA and 8 mA, a substantial portion (approximately 65–70%) of the macroions in the solution reassembled on the electrode surfaces. These images clearly illustrate the restoration of macroions on the electrode surfaces, achieved through electron exchange processes. This phenomenon results in the combination of macroions and their neutralization, leading to the formation of a composite coating on the titanium, iron plate, and rods.

Keywords: Electrospinning; electrolysis; composite coating; macroion; biopolymer.

1. Introduction

Currently, the scientific research conducted in the field of physics and nanophysics of modern materials science is aimed at creating new, unique, and special materials. Such scientific research includes the formation of nanofibers and nanofibrous materials from polymer solutions by the method of electrospinning, based on the implementation of physical processes. In recent times, an electrospinning device has been assembled in a special laboratory, with the help of which nanofibers are formed. In this research work, scientific research on the formation of layered nanofibrous non-woven materials based on local silk fibroin and acrylonitrile copolymer (AN-Co) solutions was carried out in this device.^{1,2}

[‡] Corresponding author.

In addition, obtaining surface-active coatings for specific purposes based on ionogenic polymers is one of the urgent tasks, the solution of which can be achieved by in-depth research on the movement of macroions and ions to electrodes under the influence of an electric field and their recovery on the surface of metals of various shapes.

In order to carry out the electrochemical recovery of polymers, it is necessary to prepare their polyelectrolyte solutions and to study the possibilities of moving ionogenic macromolecules as giant macroions under the influence of an electric field. These processes depend on the viscosity of ionogenic polymers depending on their molecular mass and their sensitivity to electric fields due to their ionogenic groups. Ionogenic biopolymers, including chitosan and fibroin as macroions, can shift and electrochemically recover in solutions under the influence of an electric field, as well as the possibility of forming micro and nanocoatings based on it. The unique properties of nanofibers offer innovative strategies and opportunities for sustainable energy production and creative solutions to biomedicine, and there are scientific reasons to believe that they are key factors in solving health and environmental problems.^{3,4} Nanofibers typically result in the formation of non-woven fibrous materials classified as high surface area materials due to their high surface-to-mass or volume ratio. Electrospinning technology is widely used in the preparation of a wide range of nanosized fibers for fields such as high-strength composite materials, electronic device manufacturing, drug delivery, food packaging, and membrane filtration.⁵

Electrospinning is the most widely used method due to its simplicity, low cost, potential for mass production, and the ability to control the composition and diameter of nanofibers.⁶

There is no single internationally accepted definition of nanomaterials. Indeed, they are often designed as nanoparticles, nanotubes, nanofibers, nanowires, or nanorods.⁷

Nanofibers have two similar external dimensions (nanofiber diameter = X or Y) nanoscale, while the third dimension (nanofiber length = Z) is significantly larger and there are many nanofibers⁸ and they are classified according to their nature (natural and artificial nanofibers), composition (organic, inorganic, carbon and composite nanofibers), and structure (solid, porous, non-porous, hollow) (Fig. 1).⁹

In many cases, various nanofiber production techniques can be divided into two main types: Top-down and bottom-up approaches, and bulk material nanofibers in techniques such as physico-chemical.¹⁰

Natural polymers such as collagen,¹¹ elastin,¹² and chitosan¹³ are particularly effective in the medical field of wound closure. They are biologically active in nature and can be restructured and degraded by natural mechanisms. They can also exhibit specific hemostatic and antimicrobial activity, resulting in accelerated wound healing.¹⁴

Recent studies have shown that polymer nanofibers can be designed as light-absorbing materials for solar cells. A typical polymer solar cell consists of

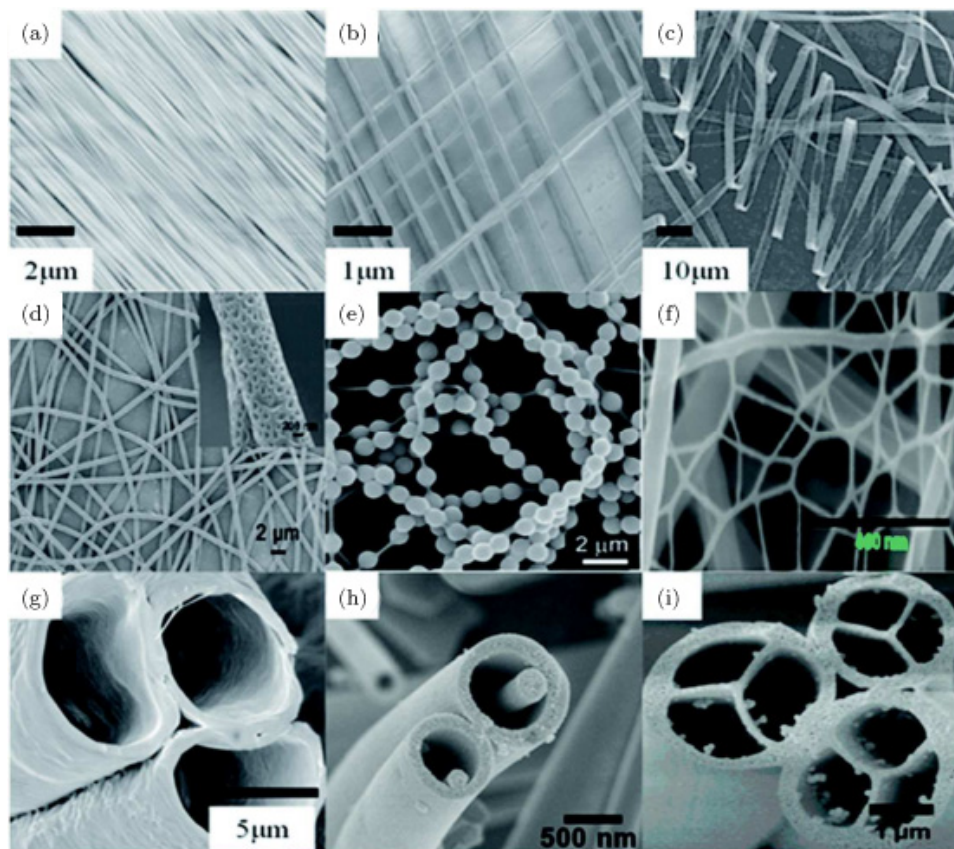


Fig. 1. (Color online) Different nanofiber morphologies. (a) Uniaxially aligned, (b) Biaxially oriented, (c) Ribbon, (d) Porous fiber, (e) Coral-like, (f) Nanowire, (g) Hollow, (h) Nanowire inside a microtube, and (i) Multichannel fiber.

three parts: (1) an anode made of indium tin oxide modified with PEDOT/polystyrene sulfonate, (2) a cathode (Al electrode), and (3) a light active layer inserted between the electrodes. Compared with silicon-based solar cells, polymer nanofiber solar cells can be lighter, cheaper, and more flexible.

p-type materials are the most promising for polymer nanofibers in the production of flexible solar cells.^{15,16} Serrano-Garcia *et al.* used the coaxial electrospinning technique to produce organic semiconducting fibers made from poly(3-hexylthiophene-2,5-diyl)/phenyl C61-butyric acid that can be used for solar cells ether (core) and PVP (shell) (Fig. 2).¹⁷

Nanosystems, including nanofibers, are structures where diameters are in nanometers and whose length is several orders of magnitude larger than their diameter. The presence and morphology of such structures are determined using electron and ultramicroscopic studies. Nanostructured materials are obtained on the basis of natural and synthetic polymers, oligomers, metals, various mixtures, and compounds.

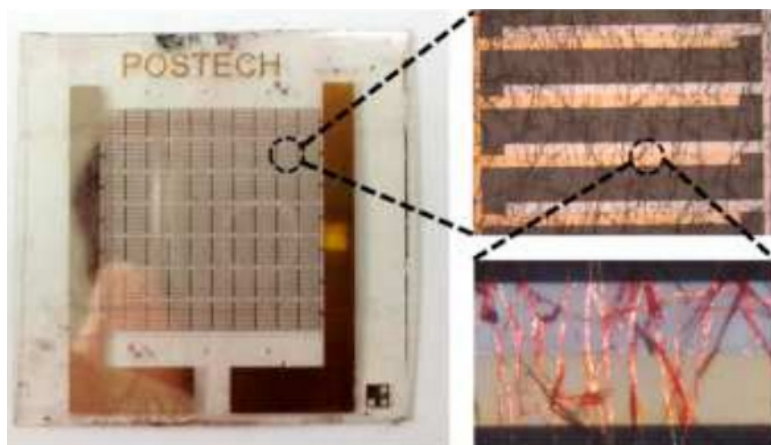


Fig. 2. (Color online) Method of coaxial electrospinning for production of organic semiconductor fibers.

The extraction of nanofibers, which are considered unique characteristics, differs from industrially produced microfibers, first of all, the diameter of the extracted fiber is required to be in the nanoscale. Therefore, the fiber-forming equipment, including the filament and the fiber-forming system and mode, is selected. There are several types of nanofiber formation, which can be conditionally divided into two groups: chemical and physical.

Fabrication of one-dimensional semiconductor materials such as TiO_2 and ZnO have been studied for various applications such as photocatalysis, dye-sensitized solar cells, gas sensors, and energy storage in Ref. 18. Various polymers such as poly(vinylpyridine), polyvinyl alcohol, polyimide are used as structural templates for the preparation of various metal-based fibers by electrospinning.¹⁹

Currently, in many countries, scientific research on the use of biopolymers in the field of medicine and their practical use is being conducted intensively. Kang, Spitzer and Poolman mentioned in their scientific work that when polyelectrolytes are subjected to external forces, including mechanical or electrical stresses, gradient fields are created²⁰ and macroions shift along the lines of force of these fields.²¹ Wang, Xu and other scientists in these fields observed that when a liquid flows from a capillary under mechanical pressure, when it is rotated using a rotor to form a stable laminar flow,²² or in the processes of electrophoresis and electrolysis, the learned ions and macroions²³ that are polarized (electrodes) are observed in the direction shift. In general, in a gradient field created under the influence of mechanical influence, macroions move along the lines of force by rotating and advancing,²⁴ while in a gradient field created under the influence of electric voltage, functional groups of macroions move towards the anode or cathode as anions or cations.²⁵ The movement of macroions in gradient fields is mentioned in the scientific articles of Li, Phan, and Schweizer, in which the reason for choosing the poles is the sensitivity of anions or cations to the effect of an electric field.²⁶

2. Research Methodology

One of the most modern methods for forming nanofibers is electrospinning, the principle basis of which was actually proposed in 1934.^{27,28} In this method, when a high-voltage direct electric field is applied along the flow of the solution, the evaporation of the solvent and the orientational joining of polymer molecules to each other and the formation of fibers at a needle tip to collector distance of 10–30 cm were observed. But the formed fibers were tangled together and had an unstable structure. By the 1990s, US scientists had seriously begun to overcome these shortcomings and create stable fibers, including nanosized fibers. Near-field electrospinning process was used for this purpose and its efficiency started a new era of obtaining polymer nanofibers which is currently developing rapidly.^{29–31}

In the electric field, the polymer coming out of the filler from the liquid-phase flow evaporates the solvent and the orientational expansion of the macromolecules forms nanofibers and falls on the screen.

The process of electrospinning involves electrostatic attraction of the flow of polymer solution coming out of the capillary (anode) to the drinker (0.1 ÷ 2.0 mm) under the influence of high voltage (0.5 ÷ 30 kV) in the air to the screen or drum (cathode) and rapid evaporation of the solvent from the flow is based on extrusion and formation of polymer molecules in the form of nanosized fiber by twisting them into an orientational state. Usually, a constant voltage of one kV per cm of the needle tip to collector distance between the anode and the cathode is intended (See Fig. 3).

In general, when the diameter of the spinneret is $d = 0.2\text{--}0.5$ mm and length $l = 2\text{--}4$ cm, if you give 1 kV of voltage for every 1 cm of the selected distance (no more than 12–15 cm) from the anode to the cathode, you can choose the most optimal condition to obtain nanofibers from a solution with $C = 10\%$ concentration of Co-AN. The change in thickness (d_n) of nanofibers can be controlled by changing r ,

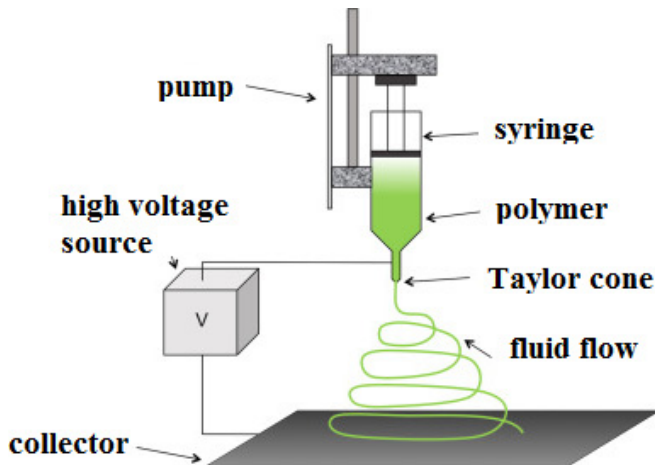


Fig. 3. (Color online) Schematic diagram of the electrospinning process.

U_{cr} , S , and C parameters. Electrospinning of nanofibers from spinning solutions of biopolymers was carried out under the action of a high voltage of 15 kV. In this case, a needle-shaped spinneret with a capillary diameter of 0.05 cm was used and the distance from the spinneret to the screen was 15 cm. Ordered uniform laying of nanofibers was carried out on the surface of the screen rotating at a frequency of 15 rpm.

The electrolysis method is very effective in creating a composite coating on the surface based on biopolymers. The main issue of the research is to determine the physical basis of creating coatings based on composite bioactive substances on the metal surface by the method of ion electrolysis and to determine the bioactive substances for them.

There are scientific grounds that phosphate, calcium, copper, gold, nickel ions, as well as chitosan, fibroin, and similar bioactive polymers–macroions can be such substances in the formation of biopolymer composite coatings. The combined use of these substances in coatings is very promising. Such an approach leads to an increase in strength and biologically active characteristics of the composite coating, in particular, on the metal surface. The main issue here is to determine the parameters of electrolysis for the formation of coatings based on the given substances. There is a great interest in the use of biopolymers that contain amino and carboxyl groups, such as chitosan and fibroin. The molecules of these biopolymers are iogenic, so they can be used as macroions; it is possible to fill them with different thicknesses using the method of electrolysis and electrochemical reduction in the metal surface.

It is also important that the bioactive polymer forms a strong coating on the metal surface, and to achieve it, it is necessary to restore multivalent ions together with macroions, that is, to use such ions as a binder in the restoration of macroions on the metal surface. Electrolysis range of direct current supplied to the metal electrode (0.1–10 mA), temperature range (30–70°C), concentrations of selected biologically active substance solutions and mixtures (0.1–10%), electrolysis time (1–20 h) were displayed.

The main focus is on the physical characteristics of the surface of metals and their smoothness and roughness. The presence of surface micro-sized roughness in metals is very important for conducting high-efficiency electrolysis and fixing the composite coatings of ions and microions with bioactive substances formed during this electrochemical recovery process.

A preliminary sketch of the electrolysis of solution ions to form a composite coating on the surface of metal plates was made (Fig. 4). In this drawing, the focus is on visual control of the electrolysis processes on the surface of the plates.

3. Results and Discussion

Electrospinning research is being carried out on the implementation of technologies for creating nanofibrous non-woven materials based on local polymer raw materials.

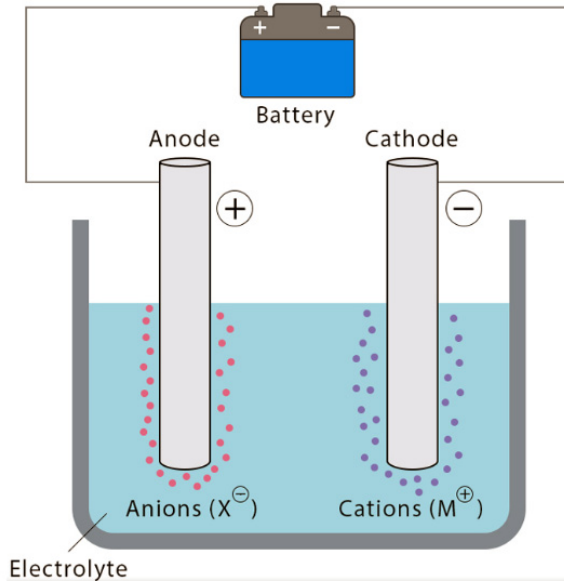


Fig. 4. (Color online) The principle diagram of the application of the electrolysis method.

These studies were carried out using the nanofiber electro spray coaxial electrospinning equipment electrospinning machine (AME-11) based on a high-tech approach (Fig. 5).

Acrylonitrile copolymer and its characteristics. The composition of acrylonitrile copolymer (AN-Co) consists of AN (93.5%), methacrylic acid (MA) (4.5%), and acrylic acid (AC) (3%), and based on it, it is known as artificial wool. Nitron fiber is obtained from it. AN:MA:AC fibers are materials with unique physical properties. They are soluble in highly concentrated (greater than 51.5%) rhodanide potassium (KaSNC) salt and in a number of organic solvents. This allows you to process them and make different products.

The average molecular weight M_η of the AN-Co is selected for research, its characteristic viscosity is measured by viscometry in dimethylformamide (DMFA) solvent $[\eta] = 454 \text{ cm}^3/\text{g}$, based on the Mark-Kunn-Hauvink equation using $[\eta] = 7.24 \cdot 10^{-2} M^{0.66}$, that is, it was determined that $M_\eta = ([\eta]/7.24 \cdot 10^{-2})^{1/0.66} = 560,000$.

Weakly concentrated ($c \approx 5 \div 10 \text{ g/dl}$) mixtures of AN-Co were used to create nanofibrous non-woven material by electrospinning.

Using this electrospinning device, the optimal conditions for obtaining nanofibers from a 10% solution of Co-AN were selected, according to which a 25 kV DC voltage was applied to the filler ($\varnothing < 1 \text{ mm}$), i.e. the anode, installed in the solution reservoir syringe, and such a voltage was under cover, nanofibers were formed at needle tip to collector distance of 12–15 cm from the filter to the screen (cathode). In this case, the diameter of the filament was 1000 times larger than the surface of the screen, and the strong electric field of the solution stream left the filament sharply separated into two

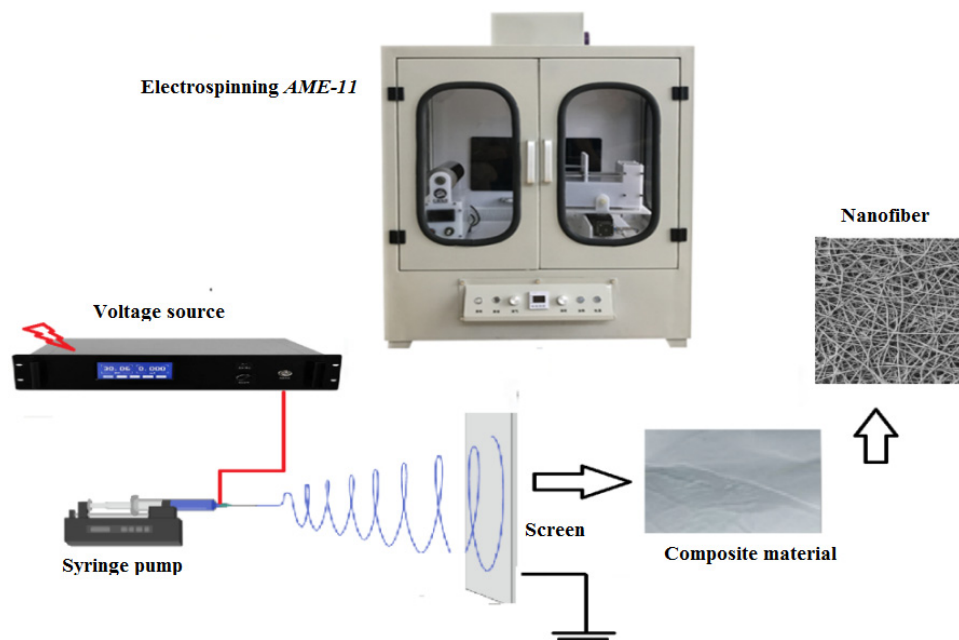


Fig. 5. (Color online) Nanofiber electro spray coaxial electrospinning equipment electrospinning machine (AME-11).

phases, i.e. the scattering of the solvent and the attraction of the polymer molecules to the screen, causing them to turn into nanosized fibers as a result of orientational crystallization. Figure 6 shows the structural arrangement of Co-AN nanofibers formed by the method of electrospinning in the nanotextile material.

Also, the resulting nanofibers were examined by atomic force microscopy; it was shown that there are nanopores on the surface of the nanofibers, which have sizes from 10 nm to 50 nm (Fig. 6).

Studies have shown that there are possibilities of nanofiber sizes and their arrangement in non-woven materials in a certain order and the formation of nanopores of specific sizes.

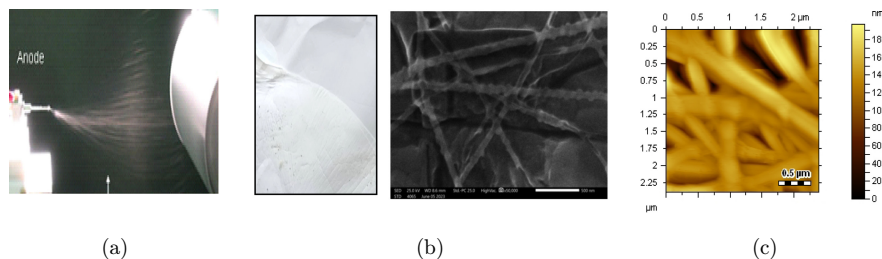


Fig. 6. (Color online) (a) Photograph of the electrospinning process of nanofiber formation. (b) Photograph and SEM image of Co-AN nanofibers as a non-woven material, and (c) atomic force microscopy image of a nanofiber.

Electrolysis. Metal plates on the surface of which microsized pits were formed by sandpaper processing, as well as metal rods with different geometric shapes, especially grooved “rods” used in technical components, were used as recovery electrodes. The recovery of macroions on such uneven surfaces is somewhat more complicated than on a smooth surface, but the recovery of macroions between pits undoubtedly leads to the formation of solid coatings.

Characterization of fibroin macromolecule. The amide group (NH_2) in the chain has a “base” character, and the carboxyl group (COON) has an “acid” character. Side radicals (R) (atom or group of atoms) has one free valence. Fibroin (FB) has 18 radicals out of a possible 20 that are clearly grouped along the chain, but their complete sequence has not been determined. Four amino acids (glycine, alanine, serine, and tyrosine) form two crystallizable sequences of up to 100 units. A single chain of fibroin has 1% positively charged, 3% negatively charged, 18% neutral, and 78% non-polar amino acid residues linked by peptide bonds. Therefore, FB is considered as a weak polyampholyte. $\text{C}_{13}\text{N}_{23}\text{N}_5\text{O}_6$ is the empirical formula of the elemental link of FB.

For conducting studies, a powdery sample of FB previously washed from natural silk fiber from sericin, oil and minerals, dissolved in CaCl_2 (50%) and precipitated in an amorphous state was used. For electrochemical recovery experiments, it is convenient to use a solution of amorphous fibroin in formic acid (HCOOH), but acidic hydrolysis is observed in this solvent. Therefore, the use of its diluted solution in water, including $\text{HCOOH}-\text{H}_2\text{O}$ (1:1), showed no additional effects, and furthermore, FB conformation strongly depends on the pH of the medium.

A dilute solution of FB was prepared in this mixed solvent and polyelectrolyte properties were studied by viscometry at 25°C . But to determine the molecular mass, 2.5 M LiCl-DMFA solvent was used, where the coefficients of the Mark-Kuhn-Hauvinck equation were found. The results of the research are presented in Fig. 7.

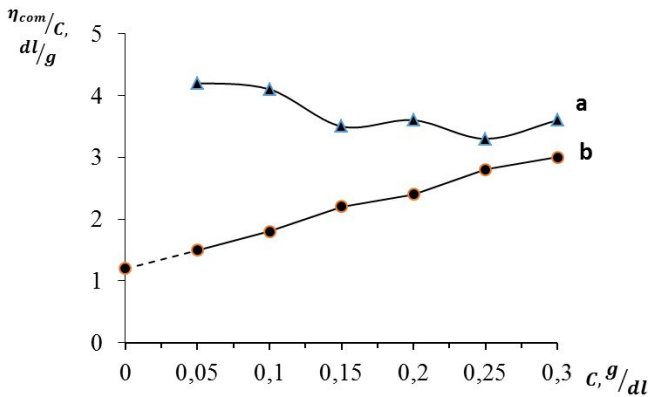


Fig. 7. (Color online) Graph of the relationship of viscosity to concentration (C): (a) FB-HCOOH: H_2O (1:1) and (b) FB-2.5 M LiCl-DMFA.

In this figure, the graph of the FB-HCOOH:H₂O (1:1) solution is curved, typical of the polyelectrolyte concentration anomaly. Therefore, the observation that the interaction of the main functional groups of FB (NH₂COOH) changes unevenly with dilution of the solution is a reason to conclude that macromolecules actively interact with the acidic environment surrounding them as macroions.

The next FB-2.5 MLiCl-DMFA solution bond graph is linear and conforms to Huggins' law. Extrapolated from it to $C \rightarrow 0$ and found that the descriptive viscosity of the $\tau_c/C = [\eta]$ condition was $[\eta] = 1.2$ dl/g. Mark-Kunn-Howing equation using FB to calculate the mean molecular mass $M_n \approx ([\eta]/1.23 \cdot 10^{-5})^{1/0.91} = 295,000$.

Tricalcium phosphate. Calcium phosphates are organic compounds of phosphoric acids containing calcium and oxygen and appear as white or colorless crystals. One of these salts is tricalcium phosphate, its chemical formula is Ca₃(PO₄)₂ and it has two modified forms: α -monoclinic (melting point >12,000°C, density 2.81 g/cm³) β -hexagonal (melting point >16,700°C, density is 3.067 g/cm³). Tricalcium phosphates Ca₃(PO₄)₂ are present in bone tissue and are part of its minerals.

A saturated solution of this compound can be obtained for electrolysis of ions. Mixtures of tricalcium phosphate with chitosan or fibroin are prepared by mixing solutions of this object. The proportions of these solutions can be controlled depending on the quality of the coating formation on the metal surface by the method of electrolysis. The presence of salt ions in polymer solutions causes them to exhibit ionic electrical conductivity.

In the electrolysis cell of the device, a $1 \times 5 \times 0.1$ cm³ titanium plate and an iron rod were used as a recovery (E_1) electrode and a graphite (E_2) sturgeon ($\emptyset 0.5$ cm) was used as an oxidation electrode. Electrochemical recovery of macroions of fibroin (a selected biopolymer) on the surface of the electrode, like metal ions, according to Faraday's law ($m = kIt$) was studied in the electrolysis device, the photo of which is shown in Fig. 7 below. Taking into account the ability of macroions to effectively move to the electrodes, experiments were conducted in diluted solutions of biopolymers with $C = 0.25$ g/dl.

The electrolysis process was carried out for 4–14 h at $I = 2$ mA, $I = 4$ mA, and $I = 8$ mA. At the end of the electrolysis time, the electrodes were kept in the cell for another 2 h in order to re-dissolve the macroions that reached the electrodes under the influence of the electric field and were not restored.

Then the electrodes were removed from the cell, dried at room temperature, and the masses before (m_1) and after (m_2) electrolysis were measured on an analytical balance with an accuracy of ± 0.0001 g, and the differences between them were found $\Delta m = m_2 - m_1$. The results are presented in Table 1.

With the movement of macroions in the electric field and their electrochemical recovery on the surface of the electrodes, the formation of metal plates and composite coatings on various shaped surfaces, their SEM images, and spectral analysis, it was found that the amount of Δm is within the range of measurement errors when the amount of current is 1 mA, and this state reaches the electrode came and showed that

Table 1. Results of recovery of macroions on electrolysis surface.

Sample	(Ti) plate–electrode			(Fe)–electrode		
	2 mA	4 mA	8 mA	2 mA	4 mA	8 mA
FB mass, Δm , g	0.071	0.084	0.102	0.075	0.092	0.105

the macroions covering it were dissolved again for 2 h after the current was cut off and that they were not electrochemically restored, i.e. the deposition of macroions on the surface of the electrode.

The electrochemical recovery of both macroions and ions together is presented in Figs. 8(a)–8(c) and the results of ZEISS SIGMA SEM 500 electron microscopic studies are presented in Fig. 6.

In the description, three characteristic areas were spectrally analyzed by the means of the AZtec program and it was determined that they belong to titanium plastic (spectrum 12) and to a mixture of FB and salt ions $\text{Ca}_3(\text{PO}_4)_2$ (tricalcium phosphate) (spectrum 66), respectively. These spectra are shown in Figs. 8(a)–8(c) in the form of spectra of dependence of the relative pulse power (imp/s/eV) on the applied power (eV). Analysis showed that 71% of spectrum 12 is Ti. In this case, it is evidence that titanium was synthesized together with other elements in nature and that it was not maximally isolated from these elements. Also, the detection of 1.7% Ca on the surface of the iron plate (spectrum 16) indicates that this ion reached the surface of titanium earlier than macroions during electrolysis and was electrochemically restored. Similarly, the analysis of spectrum 16 shows the coating composition to be 20–21% O (oxygen), 0.9–1.7% Ca (calcium), 0.3–0.4% P (phosphorus), 53% Ti (titanium) and 47% Fe (iron).

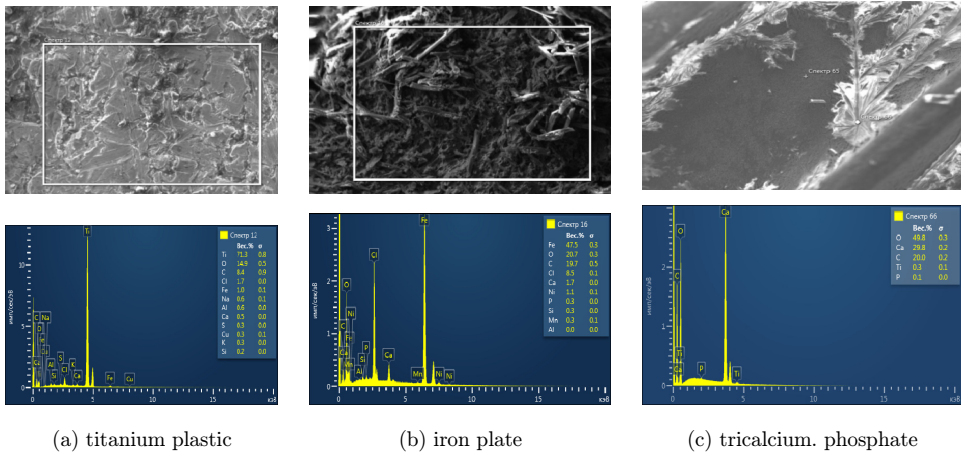


Fig. 8. (Color online) SEM images and spectral analysis of the recovery of polymer composite coatings on different surfaces.

This result indicates that $\text{Ca}_3(\text{PO}_4)_2$ is mainly recovered in this part of the composite coating. At 4 and 8 mA, macroions were restored on the surface of the electrodes, and their amount was 65–70% of the macroions in the solution. These images show that the macroions are restored on the surface of the electrode, i.e. as a result of the exchange of electrons on the surface of titanium, iron plate and rods, they combine and become neutral to form a composite coating.

4. Conclusion

In this paper, we utilized a native AN-Co solution in DMFA to produce nanofibers. These nanofibers had a thickness ranging from 50 to 200 nm. Additionally, we created layered nanofiber non-woven materials with a thickness spanning from 50 nm to 500 μm using a state-of-the-art electrospinning device. Through our analysis, we determined various key physical characteristics, including the nanopore size, which was found to be approximately 10–20 nm.

We conducted research on the electrolysis-based recovery of polymer macroions on metal surfaces, focusing on the effective implementation of the electrochemical recovery process in conjunction with macroions and their associated salt ions. During our investigation, we identified optimal conditions for this process. The concentration of biopolymer in the electrolysis device ranged from 0.04 g/dl to 0.5 g/dl. We also demonstrated the potential for creating composite coatings by varying the current in the range of 2–8 mA and adjusting the electrolysis time within the range of 4–14 h.

As a result of our research, we successfully produced composite coatings on the surfaces of titanium, iron rods, and plates. These coatings were developed using fibroin and tricalcium phosphate. We meticulously examined the microscopic characteristics of these coatings using a ZEISS SIGMA SEM 500 electron microscope. Additionally, we determined the percentage of elements restored to the surface through spectral analysis of the coating.

ORCID

B. M. Matyakubov  <https://orcid.org/0000-0001-6685-690X>

References

1. A. Barhoum, K. Pal, H. Rahier, H. Uludag, I. S. Kim and M. Bechelany, *Appl. Mater. Today* **17** (2019) 1, doi: 10.1016/j.apmt.2019.06.015.
2. K. Aruchamy, A. Mahto and S. K. Nataraj, *Nano-Struct. Nano-Objects* **16** (2018) 45, doi: 10.1016/j.nanoso.2018.03.013.
3. H. Lee, D.-N. Phan, M. Kim, D. Sohn, S.-G. Oh, S. H. Kim and I. S. Kim, *Nanomaterials* **6** (2016) 226, doi: 10.3390/nano6120226.
4. J. Jeevanandam, A. Barhoum, Y. S. Chan, A. Dufresne and M. K. Danquah, *Beilstein J. Nanotechnol.* **9** (2018) 1050, doi: 10.3762/bjnano.9.98.

5. M. S. Islam, B. C. Ang, A. Andriyana and A. M. Afifi, *SN Appl. Sci.* **1** (2019) 1248, doi: 10.1007/s42452-019-1288-4.
6. W. E. Teo and S. Ramakrishna, *Nanotechnology* **17**(14) (2006) 89, doi: 10.1088/0957-4484/17/14/R01.
7. K. S. Rho, L. Jeong, G. Lee, B.-M. Seo, Y. J. Park, S.-D. Hong, S. Roh, J. J. Cho, W. H. Park and B.-M. Min, *Biomaterials* **27**(8) (2006) 1452, doi: 10.1016/j.biomaterials.2005.08.004.
8. R. Nayak, R. Padhye, I. L. Kyratzis, Y. B. Truong and L. Arnold, *Tex. Res. J.* **82**(2) (2012) 129, doi: 10.1177/0040517511424524.
9. J. Ding and G. Wei, *RSC Adv.* **4**(94) (2014) 52598, doi: 10.1515/ntrev-2015-0065.
10. A. R. Jabur, L. K. Abbas and S. M. Muhi Aldain, *Eng. Technol. J.* **35** (2017) 340, doi: 10.30684/etj.35.4A.5.
11. S. A. Moosa, A. R. Jabur, E. S. Al-Hassani and A. M. Al-Shammari, *Eng. Technol. J.* **40**(12) (2022) 1671, doi: 10.30684/etj.2021.131990.1079.
12. A. Al-Khateeb, E. S. Al-Hassani, A. R. Jabur and S. B. A. Bakar, *Eng. Technol. J.* **41**(6) (2023) 845, doi: 10.30684/etj.2023.138439.1395.
13. B. M. Matyakubov and A. A. Kholmuminov, *Mod. Phys. Lett. B* **35**(16) (2021) 2150276, doi: 10.1142/S0217984921502766.
14. L. Buttafoco, N. G. Kolkman, P. Engbers-Buijtenhuijs, A. A. Poot, P. J. Dijkstra, I. Vermes and J. Feijen, *Biomaterials* **27**(5) (2006) 724, doi: 10.1016/j.biomaterials.2005.06.024.
15. N. Charernsriwilaiwat, P. Opanasopit, T. Rojanarata and T. Ngawhirunpat, *Int. J. Pharm.* **427**(2) (2012) 379, doi: 10.1016/j.ijpharm.2012.02.010.
16. M. Sadri, S. Arab-Sorkhi, H. Vatani and A. Bagheri-Pebdeni, *Fibers Polym.* **16** (2015) 1742, doi: 10.1007/s12221-015-5297-7.
17. W. Serrano-Garcia, S. Ramakrishna and S. W. Thomas, *Polymers (Basel)* **14**(23) (2022) 5073, doi: 10.3390/polym14235073.
18. T. G. Naghiyev, *Mod. Phys. Lett. B* **35**(6) (2021) 2150104, doi: 10.1142/S0217984921501049.
19. R. S. Madatov, F. G. Asadov, E. G. Asadov and T. G. Naghiyev, *J. Korean Phys. Soc.* **74** (2019) 508, doi: 10.3938/jkps.74.508.
20. M. A. Mahadadalkar, N. H. Park, M. Yusuf, S. Nagappan and M. Nallal, *Chemosphere* **330** (2023) 138599, doi: 10.1016/j.chemosphere.2023.138599.
21. T. G. Naghiyev, *Int. J. Mod. Phys. B* **34**(32) (2020) 2050318, doi: 10.1142/S021797922050318X.
22. M. Kim, S. B. Jo, J. H. Park and K. Cho, *Nano Energy* **18** (2015) 97, doi: 10.1016/j.nanoen.2015.10.007.
23. T. G. Naghiyev, *Int. J. Mod. Phys. B* **35**(9) (2021) 2150127, doi: 10.1142/S0217979221501277.
24. A. S. Alekperov, A. O. oglu Dashdemirov, T. Naghiyev and S. H. Jabarov, *Semiconductors* **55** (2021) 574, doi: 10.1134/S1063782621070034.
25. T. D. Ibragimov, I. S. Ramazanov, G. Kh. Guseynova, U. V. Yusifova and A. F. Nuraliyev, *UNEC J. Eng. Appl. Sci.* **2**(1) (2022) 5.
26. X. Li, Z. Zhuang, D. Qi and C. Zhao, *Sens. Actuators B, Chem.* **330** (2021) 129239, doi: 10.1016/j.snb.2020.129239.
27. A. A. Kholmuminov, B. M. Matyakubov and T. T. Rakhmonov, *Chem. Mater. Sci. Res. J.* **3**(2) (2021) 15, doi: 10.51594/cmsrj.v3i2.216.
28. K. Yang, X. Chu, X. Zhang, X. Li, J. Zheng, S. Li, N. Li, T. A. Sherazi and S. Zhang, *J. Membr. Sci.* **603** (15) (2020) 118025, doi: 10.1021/acsam.9b00674.

J. M. Khakkulov et al.

29. J. Khakkulov, Z. Temirov and S. Khalilov, *Am. J. Appl. Sci.* **3**(6) (2021) 34, doi: 10.37547/tajas/Volume03Issue06-06.
30. A. D. Phan and K. S. Schweizer, *ACS Macro Lett.* **9**(4) (2020) 448, doi: 10.1021/acsmacrolett.0c00006.
31. D. Li and Y. Xia, *Adv. Mater.* **16**(14) (2004) 1151, doi: 10.1002/adma.200400719.